Control of transient chaos in tent maps near crisis. II. Periodic orbit targeting

C. M. Place and D. K. Arrowsmith
Mathematics Research Centre, Queen Mary and Westfield College, University of London, London E1 4NS, United Kingdom
(Received 23 August 1999)

Recent work on a symbolic approach to the calculation of probability distributions arising in the application of the Ott-Grebogi-Yorke strategy to transiently chaotic tent maps is extended to the case of control to a nontrivial periodic orbit. Closed forms are derived for the probability of control being achieved and the average number of iterations to control when it occurs. Both single-component and multiple-component targeting are considered, and illustrative examples of the results obtained are presented.

PACS number(s): 05.45.−a

I. INTRODUCTION

In earlier work [1] the problem of using the Ott-Grebogi-Yorke (OGY) strategy to control the orbits of a transiently chaotic tent map to its nontrivial fixed point was considered. A numerical experiment was envisaged in which initial points were chosen at random (i.e., according to a uniform distribution) in [0,1] and the probability that the OGY target interval was reached in less than or equal to a chosen number of iterations was obtained. A symbolic dynamic approach was adopted that allowed the probability distributions associated with such an experiment to be obtained in closed form and the results were interpreted in relation to the work of Tél [2].

In order to extend the symbolic analysis used in [1] to the case of OGY control to nontrivial periodic orbits, it is important to be clear about the details of the numerical experiment that is to be treated. For example, control to a period-q orbit of a map $T:\mathbf{R}\rightarrow\mathbf{R}$, could be achieved by taking a target interval around one of the fixed points of the qth power of the map and generating the orbits of randomly chosen initial points under T^q until the target interval is reached. Such an experiment involves different probability distributions from one in which a target interval is chosen around the same period-q point but the iterates of initial points under the map T itself are considered (cf. [3,4]). Since T^q is commonly obtained by making q iterations of T, it would seem to be perverse to check if the target interval had been reached only at every qth iterate. However, even if checks are made at each iterate, the procedure relies upon reaching the periodic orbit via a ''single-component'' target. From a symbolic standpoint, such an experiment is similar to the fixed point problem (see [1]) in that only a single binary string is to be avoided during preimage construction.

The symbolic approach lends itself naturally to dealing with an alternative experiment in which the target is taken to be a union of q disjoint intervals, each of which contains one, and only one, of the periodic points that make up the period-q orbit, i.e., the target consists of q disjoint components. In such a ''multiple-component'' experiment, the period-q orbit can be reached through q disjoint target components each containing one of its periodic points. The numerical experiment considered takes a randomly chosen initial point in [0,1] and obtains the probability that its orbit first reaches *any* one of the q components of the target union. In symbolic terms, the single code block describing the target interval for the fixed point in [1] is replaced by q code blocks representing the q components of the target union for the periodic orbit. In order to ensure that only first entries into *any* component are counted, it is necessary to avoid occurrences of q code blocks in the preimage formation process.

As in the fixed point case, the symbolic approach places some limitations on the choice of target intervals. In particular, for multiple-component targets, the requirement that each component of the target union contains one and only one period-q point imposes stronger constraints than in the fixed point case. For example, if a minimum of one symbolic period of the orbit is used to define each target interval then the maximum length of each component of the target union is 2^{-q}. This constraint also applies to the single-component target if the periodic orbit under consideration is to be clearly identified or if comparisons of the distributions for the q possible choices of single target are to be made.

It should be noted that the present discussion is concerned only with the probability that iterates of the map itself first enter the chosen target (i.e., stage 1 of the OGY control procedure). When the orbit is inside the target, the control is applied (stage 2 of the OGY method) so as to ensure that the orbit of the controlled system remains close to the period-q orbit. The latter phase of the control process is not considered in this paper. It is assumed that once the target has been entered control can be maintained.

II. NUMBERS OF FIRST-ENTRY PREIMAGES

The results for the single-component target are contained, as a special case, within the analysis of the multiple-component experiment and, therefore, the latter is presented first.

A. Multiple-component targeting

The numbers of first-entry preimages of each component of the target union for a period-q orbit can be obtained by using combinatorial arguments similar to those discussed by Odlyzko [5] and developed in greater depth by Guibas and Odlyzko [6]. The latter reference contains an intriguing collection of applications of the same type of string counting:

TABLE I. Decomposition of the $\{K_i = BA_i | B$ counts for $f_{L_q}(m)\}$ according to the position of the possible occurrence of elements of L_q. The index j appearing in this table can take any of the values $1, \ldots, q$.

Type of K_i	No. of type	Condition for convergence	s
$b_1 b_2 \ldots b_m A_i$	$h_{L_q}(j, m+r)$	$a_1^{(i)} a_2^{(i)} \ldots a_r^{(i)} = a_1^{(j)} a_2^{(j)} \ldots a_r^{(j)}$	0
$b_1 b_2 \ldots b_{m-1} A_j a_r^{(i)}$	$h_{L_q}(j, m+r-1)$	$a_1^{(i)} a_2^{(i)} \ldots a_{r-1}^{(i)} = a_2^{(j)} a_3^{(j)} \ldots a_r^{(j)}$	1
$b_1 b_2 \ldots b_{m-2} A_j a_{r-1}^{(i)} a_r^{(i)}$	$h_{L_q}(j, m+r-2)$	$a_1^{(i)} a_2^{(i)} \ldots a_{r-2}^{(i)} = a_3^{(j)} a_4^{(j)} \ldots a_r^{(j)}$	2
$\vdots$	$\vdots$	$\vdots$	$\vdots$
$b_1 b_2 \ldots b_{m-r+1} A_j a_2^{(i)} \ldots a_r^{(i)}$	$h_{L_q}(j, m+1)$	$a_1^{(i)} = a_r^{(j)}$	$r-1$

from coin-tossing games, through clustering problems, to prefix-synchronized codes and pattern matching algorithms.

1. The string counting problem

Let $A_i = (.a_1^{(i)} a_2^{(i)} \ldots a_r^{(i)})$, $i = 1, \ldots, q$, be the code blocks representing the q components of the target union for the period-q orbit under consideration, and let $L_q = \{A_i | i = 1, \ldots, q\}$ be the list of representatives of the target union. In order to construct first-entry preimage codes for the target union, each element of L_q must be considered in turn. Recall that, since the tent map T_ν is conjugate to a leftshift on infinite binary sequences, the preimages of such an element are constructed by repeatedly adding 0 or 1 to its left-hand end and counting only those resulting codes for which no element of L_q appears in the leftmost r positions. It follows that, for a particular element A_i of L_q, first-entry preimage codes of order k are binary strings of length $m = k + r$, which have A_i at their right-hand end but do not contain any element of L_q, as a substring of r adjacent characters, elsewhere in them. Since the elements of L_q are distinct, so are their preimage codes, and therefore the set of order-k, first-entry preimage codes for the target union is the disjoint union of those for the individual elements of L_q.

Define (a) $f_{L_q}(m)$ to be the number of binary strings of length m that do not contain any of the elements of L_q as substrings of r adjacent characters within them; and (b) $h_{L_q}(j, m)$ to be the number of binary strings of length m with A_j at their right-hand end but with no A_i, $i = 1, \ldots, q$, occurring as a substring of r adjacent characters elsewhere in them.

Let $B = (.b_1 b_2 \ldots b_m)$ be counted for $f_{L_q}(m)$ and observe that the string $b_1 b_2 \ldots b_m b$, where b is either 0 or 1, is a string of length $m+1$ that has one (and only one) of the following properties: (0) it contains none of the elements of L_q; (1) it contains A_1 with $A_1 = b_{m-r+2} \ldots b_m b$; (2) it contains A_2 with $A_2 = b_{m-r+2} \ldots b_m b$; $\ldots$; (q) it contains A_1 with $A_q = b_{m-r+2} \ldots b_m b$. The strings appearing in properties (1), $\ldots$, (q) have an element of L_q at their right-hand end but there are no other occurrences of any of these substrings elsewhere in the concatenation Bb. It follows that

$$2 f_{L_q}(m) = f_{L_q}(m+1) + \sum_{i=1}^{q} h_{L_q}(i, m+1). \tag{2.1}$$

Now consider the concatenation $K_i = BA_i$, for any choice of $i = 1, \ldots, q$. Clearly, there are precisely $f_{L_q}(m)$ such concatenations for each i, because there is one for every possible B. However, the number of concatenations K_i can be counted in another way. Although B does not contain any element of L_q as a substring, K_i can contain such substrings as shown in the first column of Table I.

Every K_i must belong to one, and only one, of the types specified and, consequently, the total number of K_i is the sum of the numbers of each type of K_i that occurs. The number of each type of K_i is given in the second column of Table I. However, a particular type of K_i occurs if and only if the condition given in the third column of the table is satisfied. These conditions can be represented by indicator functions $c_{ij}(s)$ defined, for $i, j = 1, \ldots, q$, by

$$c_{ij}(s) = \begin{cases} 1 & \text{if } a_1^{(i)} a_2^{(i)} \ldots a_{r-s}^{(i)} = a_{s+1}^{(i)} a_{s+2}^{(i)} \ldots a_r^{(i)} \\ 0 & \text{otherwise,} \end{cases} \tag{2.2}$$

with $s = 0, 1, \ldots, r-1$. It follows that, for each $i = 1, \ldots, q$,

$$f_{L_q}(m) = \sum_{j=1}^{q} \sum_{s=0}^{r-1} c_{ij}(s) h_{L_q}(j, m+r-s). \tag{2.3}$$

2. Generating functions

Generating functions for the numbers of binary strings of given length that have the above properties can be obtained as follows. Multiplication of Eqs. (2.1) and (2.3) by z^m, and summation over m from zero to infinity, can be shown to yield the following relationships between the generating functions $F_{L_q}(z)$ and $H_{L_q}^{(j)}(z)$ for the numbers $f_{L_q}(m)$ and $h_{L_q}(j, m)$, $j = 1, \ldots, q$, respectively. Equation (2.1) gives

$$2F_{L_q}(z) = z^{-1}(F_{L_q}(z) - 1) + z^{-1} \sum_{i=1}^{q} H_{L_q}^{(i)}(z), \tag{2.4}$$

and, for $i = 1, \ldots, q$, Eq. (2.3) leads to

$$F_{L_q}(z) = z^{-r} \sum_{j=1}^{q} C_{ij}(z) H_{L_q}^{(j)}(z), \tag{2.5}$$

where the coefficient

$$C_{ij}(z) = \sum_{s=0}^{r-1} c_{ij}(s) z^s \tag{2.6}$$

is the correlation polynomial for the strings A_i and A_j (cf. Odlyzko [5]). Elimination of $F_{L_q}(z)$ from Eq. (2.4) by using Eq. (2.5) results in a set of q linear equations, with polyno-

mial coefficients, for the unknown generating functions $H_{L_q}^{(j)}(z)$, $j=1,\ldots,q$. More precisely, for $i=1,\ldots,q$,

$$\sum_{j=1}^{q} \pi_{ij}(z) H_{L_q}^{(j)}(z) = z^r, \tag{2.7}$$

where

$$\pi_{ij}(z) = (1-2z)C_{ij}(z) + z^r. \tag{2.8}$$

These equations have a unique solution provided that the coefficient matrix is nonsingular over the field of rational functions.

Observe that the numbers $h_{L_q}(j,m)$ obtained from the expansion of the rational function $H_{L_q}^{(j)}(z)$ are zero for $m<r$, for any j (there are no strings satisfying the defining property of length less than r) and the number of first-entry preimages of A_j of order k is given by $h_{L_q}(j,k+r)$. Moreover, the total number of order-k, first-entry preimages for the period-q orbit contained in the target union is given by

$$N_k^{(r)}(L_q) = \sum_{j=1}^{q} h_{L_q}(j,k+r). \tag{2.9}$$

These numbers can be obtained directly from a generating function $H_{L_q}(z)$ that is the sum over j of the generating functions $H_{L_q}^{(j)}(z)$.

B. Single-component targeting

Corresponding results to those given in Sec. II A can be obtained for the single-component target by replacing the list L_q in the multiple-component analysis by the particular code block A_i representing the single target interval. Of course, any of the q members of the list L_q can be chosen for this purpose. Apart from its effect on the definitions of the binary strings involved in the first-entry preimage codes, this change simply removes the summations over the elements of L_q in the key results (2.1) and (2.3). These equations are replaced by

$$2f_{A_i}(m) = f_{A_i}(m+1) + g_{A_i}(m+1) \tag{2.10}$$

and

$$f_{A_i}(m) = \sum_{s=0}^{r-1} c_{ii}(s) g_{A_i}(m+r-s), \tag{2.11}$$

respectively. In Eqs. (2.10) and (2.11) g has been used instead of h to emphasize that the strings involved must avoid only the single code block A_i, and not the whole list L_q. It is therefore appropriate to use the same notation as was used in [1] for the fixed point case. Indeed, the fixed point problem corresponds to Eq. (2.11) with $c_{ii}(s)=1$, for $s=0,1,\ldots,r-1$. Multiplication of Eqs. (2.10) and (2.11) by z^m, and summation over m from zero to infinity, can be shown to yield

$$(1-2z)F_{A_i}(z) + G_{A_i}(z) = 1 \tag{2.12}$$

and

$$F_{A_i}(z) = z^{-r} C_{A_i}(z) G_{A_i}(z), \tag{2.13}$$

where

$$C_{A_i}(z) = \sum_{s=0}^{r-1} c_{ii}(s) z^s. \tag{2.14}$$

Here $F_{A_i}(z)$ and $G_{A_i}(z)$ are the generating functions for the numbers $f_{A_i}(m)$ and $g_{A_i}(m)$, respectively, and $C_{A_i}(z)$ is the correlation polynomial for the target string A_i with itself (see Odlyzko [5]). Substitution of Eq. (2.13) into Eq. (2.12) gives

$$G_{A_i}(z) = \sum_{m=0}^{\infty} g_{A_i}(m) z^m = \frac{z^r}{\{(1-2z)C_{A_i}(z) + z^r\}}. \tag{2.15}$$

The numbers $g_{A_i}(m)$ are zero for $m<r$ and $g_{A_i}(r)=1$ (there is precisely one string of length r with A_i at its right-hand end and none of length less than r) and the number of first-entry preimages of A_i of order k, $N_k^{(r)}(A_i)$, is $g_{A_i}(k+r)$.

III. CALCULATION OF PROBABILITIES

A. Successful control for a multiple-component target

For the hypothetical numerical experiment described in Sec. I, the probability of achieving control to the period-q orbit is given by the total length of the first-entry preimages contributing to the particular event considered. For example, control in less than or equal to n iterations of the map occurs with probability $p_{L_q}(\nu,r;n)$ given by

$$\sum_{k=0}^{n} N_k^{(r)}(L_q)(2\nu)^{-(k+r)} = \sum_{k=0}^{n}\sum_{j=1}^{q} h_{L_q}(j,k+r)(2\nu)^{-(k+r)} = \sum_{m=0}^{n}\sum_{j=1}^{q} h_{L_q}(j,m)(2\nu)^{-m}. \tag{3.1}$$

This follows because the q components of the target union all have length $(2\nu)^{-r}$ and the process of taking preimages reduces the lengths of these components by a factor of 2ν for each unit increase in order. Recall that $h_{L_q}(j,m)=0$ for $m<r$ and $j=1,\ldots,q$. In the limit of arbitrarily large n, Eq. (3.1) gives the probability $p_{L_q}(\nu,r)$ that control is ultimately achieved with the target union L_q. The result is

$$p_{L_q}(\nu,r) = \lim_{n\to\infty}[p_{L_q}(\nu,r;n)] = \sum_{j=1}^{q} H_{L_q}^{(j)}((2\nu)^{-1}) = H_{L_q}((2\nu)^{-1}). \tag{3.2}$$

A valuable check on the expressions for the generating functions $H_{L_q}^{(j)}(z)$, obtained by solution of Eq. (2.7) is that $p_{L_q}(1,r)=1$. This must be the case because, for $\nu=1$, the orbits of all points remain in $[0,1]$ indefinitely and, with

probability 1, the orbit of any choice of initial point will ultimately reach one of the components of the target union (cf. [1], Sec. IV A).

B. Failure of control for a multiple-component target

The binary strings that count for $f_{L_q}(m)$ are of length m and do not contain any element of the set L_q. When $\nu>1$, each such string represents a subinterval of [0,1], of length $(2\nu)^{-m}$, containing points with orbits that do not encounter any member of the target union in m iterations. Such a subinterval contains points of two distinct types. Each subinterval can be disjointly decomposed into a preimage [of length $(1-\nu^{-1})(2\nu)^{-m}$] of the escape interval I_E made up of points [of type (i)] whose orbits leave [0,1] in $m+1$ iterations without being controlled; and the complement in the subinterval [of length $\nu^{-1}(2\nu)^{-m}$] of this preimage of I_E, made up of points [of type (ii)] whose fate is not decided in n iterations. It follows that

$$\overline{p}_{L_q}(\nu,r;n)=(1-\nu^{-1})\sum_{m=0}^{n} f_{L_q}(m)(2\nu)^{-m} \tag{3.3}$$

is the probability that the orbit of a randomly chosen initial point will enter I_E, without passing through the target union, in less than or equal to n iterations of T_ν. Thus Eq. (3.3) gives the probability of selecting an initial point [of type (i)] for which it is clear after n iterations that control will never be achieved. In the limit in which n becomes arbitrarily large, the contribution from points of type (ii) must tend to zero. This is the case because, for $\nu>1$, almost all (in the sense of Lebesgue measure) initial points have orbits that ultimately leave [0,1] and, for sufficiently large n, the fate (i.e., whether its orbit is controlled or not) of almost every point must be determined. It can therefore be concluded that

$$\overline{p}_{L_q}(\nu,r)=(1-\nu^{-1})F_{L_q}((2\nu)^{-1}) \tag{3.4}$$

is the probability that the orbit of a randomly chosen initial point will never be controlled. Moreover, the interpretation of the generating functions given in Eqs. (3.2) and (3.4) is confirmed by Eq. (2.4), which can be written in the form

$$H_{L_q}((2\nu)^{-1})+(1-\nu^{-1})F_{L_q}((2\nu)^{-1})=1, \tag{3.5}$$

so that $p_{L_q}(\nu,r)+\overline{p}_{L_q}(\nu,r)$ is equal to unity, as required. Observe that $\overline{p}_{L_q}(1,r)=0$, so that control is always achieved when $\nu=1$. For finite n, there is a nonzero probability $u_{L_q}(\nu,r;n)$ that the fate of the initial point is undecided in less than or equal to n iterations, and then

$$p_{L_q}(\nu,r;n)+u_{L_q}(\nu,r;n)+\overline{p}_{L_q}(\nu,r;n)=1. \tag{3.6}$$

C. Outcomes for a single-component target

Similar arguments can be used to derive analogous probabilities of success or failure of control for the single-component target experiment. The probabilities for successful control corresponding to Eqs. (3.1) and (3.2) are

$$\begin{aligned} p_{A_i}(\nu,r;n)&=\sum_{k=0}^{n} N_k^{(r)}(A_i)(2\nu)^{-(k+r)} \\ &=\sum_{k=0}^{n} g_{A_i}(k+r)(2\nu)^{-(k+r)} \\ &=\sum_{m=0}^{n} g_{A_i}(m)(2\nu)^{-m} \end{aligned} \tag{3.7}$$

and

$$p_{A_i}(\nu,r)=\lim_{n\to\infty}[p_{A_i}(\nu,r;n)]=G_{A_i}((2\nu)^{-1}), \tag{3.8}$$

respectively; while

$$\overline{p}_{A_i}(\nu,r;n)=(1-\nu^{-1})\sum_{m=0}^{n} f_{A_i}(m)(2\nu)^{-m}, \tag{3.9}$$

$$\overline{p}_{A_i}(\nu,r)=(1-\nu^{-1})F_{A_i}((2\nu)^{-1}), \tag{3.10}$$

and

$$G_{A_i}((2\nu)^{-1})+(1-\nu^{-1})F_{A_i}((2\nu)^{-1})=1 \tag{3.11}$$

replace Eqs. (3.3), (3.4), and (3.5). Here Eq. (3.11) follows directly from Eq. (2.12) with $z=(2\nu)^{-1}$. The analogous result to Eq. (3.6) simply has A_i rather than L_q labeling the probabilities involved.

IV. RECURRENCE RELATIONS

The generating functions obtained in Sec.II provide a practical means of calculating the limiting probabilities, defined in Sec. III, as functions of ν and r. However, the expansion of the appropriate generating function in powers of z does not lead to a particularly efficient algorithm for obtaining the numbers of first-entry preimages needed to compute the probability of success or failure of control in less than or equal to a finite number n of time steps. Such computations are best performed with the aid of the corresponding recurrence relation. These relations are contained in the fundamental equations: (2.1) and (2.3) for the multiple-component target and (2.10) and (2.11) for the single-component experiment.

A. Multiple-component target

Equation (2.3) gives, for each $i=1,\ldots,q$,

$$\begin{aligned} f_{L_q}(k+1)&=\sum_{j=1}^{q}\left\{c_{ij}(0)h_{L_q}(j,k+1+r)\right. \\ &\qquad\left.+\sum_{s=1}^{r-1} c_{ij}(s)h_{L_q}(j,k+r-(s-1))\right\} \\ &=h_{L_q}(i,k+1+r) \\ &\qquad+\sum_{j=1}^{q}\sum_{s=0}^{r-2} c_{ij}(s+1)h_{L_q}(j,k+r-s), \end{aligned} \tag{4.1}$$

since $c_{ij}(0)=\delta_{ij}$, the Kronecker δ function. Substitution of Eq. (4.1) into Eq. (2.1) (with m replaced by k) then yields

$$\begin{aligned} h_{L_q}(i,k+r+1)=&\sum_{j=1}^{q}\left\{2\sum_{s=0}^{r-1}c_{ij}(s)h_{L_q}(j,k+r-s)\right. \\ &-\sum_{s=0}^{r-2}c_{ij}(s+1)h_{L_q}(j,k+r-s) \\ &\left.-h_{L_q}(j,k+1)\right\} \\ =&\sum_{j=1}^{q}\sum_{s=0}^{r-1}[2c_{ij}(s)-c_{ij}(s+1)] \\ &\times h_{L_q}(j,k+r-s), \end{aligned} \tag{4.2}$$

where $c_{ij}(r)=1$. Equation (4.2), with $m=k+r$, provides an expression for $h_{L_q}(j,m+1)$ in terms of $h_{L_q}(j,l)$ with $j=1,\ldots,q$ and $l=m,m-1,\ldots,m-r+1$. Given that $h_{L_q}(j,m)=0$ for $m<r$ and $h_{L_q}(j,r)=1$, for $j=1,\ldots,q$, Eq. (4.2) allows $h_{L_q}(i,m)$, $i=1,\ldots,q$, to be generated for $m>r$ provided that the correlation coefficients are known. Note that the integer variable k in Eq. (4.2) corresponds to the order of the preimage of the target component under T_ν.

B. Single-component target

When the corresponding arguments are applied to Eqs. (2.10) and (2.11), the result is

$$g_{A_i}(m+1)=\sum_{s=0}^{r-1}[2c_{ii}(s)-c_{ii}(s+1)]g_{A_i}(m-s), \tag{4.3}$$

where $c_{ii}(r)=1$, $g_{A_i}(r)=1$, and $g_{A_i}(m)=0$, for $m=1,\ldots,r-1$. For a particular choice of the code block A_i, the correlation coefficients can be calculated and Eq. (4.3) allows the numbers of first-entry preimages of order $k=m-r$ to be obtained for the corresponding target interval.

C. Correlations

In comparing Eqs. (4.2) and (4.3), it is important to note that the latter contains no cross correlations: only the correlation coefficients of the target string with itself are involved. On the other hand, Eq. (4.2) shows that, for the multiple-component target, the numbers of first-entry preimages of each member of the target union involve the correlation coefficients of its code block with every member of the list L_q. It follows that, for the single-component target, the recurrence relation involves only numbers of first-entry preimages of the target interval itself. In contrast, the recurrence relation for a particular component of the multiple-component target additionally involves such numbers for other components of the target union. It is perhaps worth noting that Eq. (4.2) only provides a stepping stone to the real objective in the multiple-component experiment, namely, $N_k^{(r)}(L_q)=\sum_{j=1}^{q}h_{L_q}(j,k+r)$, the number of order-$k$, first-entry preimages to the target union as a whole.

D. Probability distributions for finite numbers of iterations

The recurrence relations developed above allow calculation of probabilities such as $p_{L_q}(\nu,r;n)$, $u_{L_q}(\nu,r;n)$, and $\overline{p_{L_q}}(\nu,r;n)$ for chosen values of n, without recourse to the expansion of the rational form $H_{L_q}(x)$ to obtain the numbers $N_k^{(r)}(L_q)$ for $k=0,1,\ldots,n$. Even for the single-component target, where the generating functions are easily obtained, it is more convenient to compute $p_{A_i}(\nu,r;n)$, $u_{A_i}(\nu,r;n)$, and $\overline{p_{A_i}}(\nu,r;n)$ from the recurrence relation.

V. AVERAGE NUMBER OF ITERATIONS TO CONTROL

A. Multiple-component experiments

In [1], the generating function $\hat{G}_r(z)$ for the numbers of first-entry preimages of the target interval was used to obtain the average number of iterations for control to be achieved, given that the orbit of the initial point was controlled. In order to carry out the equivalent derivation for a period-q orbit with multiple-component targeting, it is convenient to extract a corresponding quantity, $\hat{H}_{L_q}(z)$, from the rational generating function $H_{L_q}(z)$ defined in Eq. (3.2). Recall that $h_{L_q}(j,m)=0$, for $m=0,1,\ldots,r-1$, because there are no binary strings of length less than r digits that contain any element of L_q. Thus

$$H_{L_q}(z)=\sum_{m=0}^{\infty}\left[\sum_{j=1}^{q}h_{L_q}(j,m)\right]z^m=z^r\hat{H}_{L_q}(z), \tag{5.1}$$

where

$$\begin{aligned} \hat{H}_{L_q}(z)=&z^{-r}\sum_{m=r}^{\infty}\left[\sum_{j=1}^{q}h_{L_q}(j,m)\right]z^m \\ =&\sum_{k=0}^{\infty}nty\left[\sum_{j=1}^{q}h_{L_q}(j,k+r)\right]z^k \\ =&\sum_{k=0}^{\infty}N_k^{(r)}(L_q)z^k. \end{aligned} \tag{5.2}$$

A similar argument to that used in [1] can be applied to Eq. (5.2) to show that the average number of iterations to control is given by

$$\tau_{L_q}(\nu,r)=\left[\frac{z\hat{H}'_{L_q}(z)}{\hat{H}_{L_q}(z)}\right]_{z=(2\nu)^{-1}}. \tag{5.3}$$

Equation (5.3) provides the limiting value of the average number of iterations to control, when control occurs, that should be obtained from experiments that admit arbitrarily large numbers of iterations for each member of an arbitrarily large sample of initial points. The recurrence relations, given in Sec. IV, allow the more practical estimates,

$$\tau_{L_q}(\nu,r;n)=\frac{\sum_{k=1}^{n} kN_k^{(r)}(L_q)(2\nu)^{-(k+r)}}{\sum_{k=0}^{n} N_k^{(r)}(L_q)(2\nu)^{-(k+r)}}, \qquad (5.4)$$

to be computed for any chosen n. These quantities give valuable information about how quickly the large-n limit is approached for different choices of ν and r.

B. Single-component experiments

In such an experiment, the calculation of the average number of iterations to control, given that control takes place, is formally the same as that presented in [1] for the fixed point target, except that the recurrence relation and the generating function are determined by the target interval code block A_i rather than $(.11\ldots1)_r$. The lack of cross correlations means that the analysis is considerably simpler than the multiple-component case using the same value of r. It follows that it is easier to study the q and r dependence of τ using this kind of experiment. The equivalent results to Eqs. (5.1)–(5.4), for the single-component target, can be obtained by making the following notational changes: $H\to G$, $L_q\to A_i$, $h\to g$, $(j,m)\to(m)$, and $(j,k+r)\to(k+r)$, and $\Sigma_{j=1}^{q}$ no longer appears.

VI. DISCUSSION—SINGLE-COMPONENT TARGETS

The purpose of this section is to highlight some of the features of control to a nontrivial periodic orbit that follow from the above analysis.

A. Some overall limits on the probability of successful control

The analysis of the single-component experiment for a nontrivial period-q orbit is formally similar to the treatment of the fixed point problem, but differs from it in the correlation coefficients that are involved. In the fixed point case, the pattern of these coefficients with increasing r is particularly simple because they are all equal to unity (see Sec. II B). When the code block representing the target interval is no longer simply $(.11\ldots1)_r$, less trivial patterns of correlation coefficients emerge. However, Eq. (2.15) shows that the generating function does not depend strongly on the variations in correlation coefficients that may arise.

Recall that, for a given value of r, the correlation polynomial is of degree at most $(r-1)$ and has coefficients that are either 0 or 1. Moreover, since only correlations of the target string with itself are involved in the single-component experiment, the coefficient of z^0 must be unity. It follows that the correlation polynomial for any target block of length r lies between the extreme cases

$$C_0(z)\equiv 1 \text{ and } C_1(z)=1+z+\cdots+z^{r-1}=(1-z^r)/(1-z). \qquad (6.1)$$

Consequently, the generating function given in Eq. (2.15) has upper and lower limits of

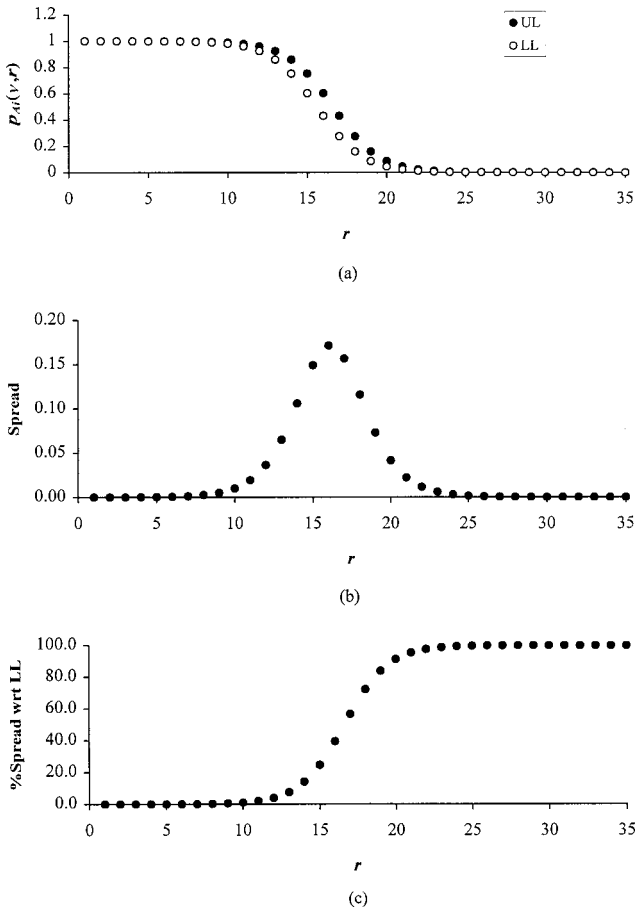

FIG. 1. Illustration of the r dependence of the limits to the probability of successful control for $z=1/(2\nu)$ with $\nu=1.000\,01$: (a) plots of the limits given by Eq. (6.3); (b) the spread of possible values given by Eq. (6.4); (c) the spread of possible values expressed as a percentage of the lower limit (LL).

$$G_{UL}^{(r)}(z)=z^r\{(1-2z)C_0(z)+z^r\}^{-1} \text{ and}$$
$$G_{LL}^{(r)}=z^r\{(1-2z)C_1(z)+z^r\}^{-1}. \qquad (6.2)$$

It follows that the probability of successful control satisfies

$$G_{LL}^{(r)}((2\nu)^{-1})\leqslant p_{A_i}(\nu,r)\leqslant G_{UL}^{(r)}((2\nu)^{-1}), \qquad (6.3)$$

for any target string A_i of length r.

The limits of the probability of successful control given by Eq. (6.3) are plotted in Fig. 1(a) as a function of the target string length r for $\nu=1.000\,01$. The difference

$$G_{UL}^{(r)}((2\nu)^{-1})-G_{LL}^{(r)}((2\nu)^{-1})=\left[\frac{z^{r+1}(1-2z)(1-z^{r-1})}{(1-2z+z^r)(1-2z+z^{r+1})}\right]_{z=(2\nu)^{-1}} \qquad (6.4)$$

is a measure of the spread of possible values for the probability of control taking place. In general, as illustrated in Fig. 1(b), this spread passes through a well-defined maximum for $r=r_c$, given by

$$r_c=\left\lceil 1+\left[\ln\left\{\frac{(1-2z)(1-z)}{(1-2z+z^3)}\right\}\Big/\ln(z)\right]_{z=(2\nu)^{-1}}\right\rceil, \tag{6.5}$$

where $\lceil * \rceil$ is the smallest integer greater than or equal to *.

It would be wrong to conclude that correlation variations have a significant effect on $p_{A_i}(\nu,r)$ only for values of r lying within the peak in the spread of its possible values. For values of r lying below the peak, both limits are close to unity and the spread is genuinely of little significance; but for values of r above the peak both limits are near to zero and the spread of possible values can represent very significant relative differences in the probability of successful control. For example, with $(2\nu)^{-1}=2^{-1}(1-\delta)$ and $2^{-r}\ll\delta\ll 1$, the limits given in Eq. (6.3) yield

$$\frac{1}{2}\frac{(2\nu)^{-r}}{\delta}<p_{A_i}(\nu,r)\leqslant\frac{(2\nu)^{-r}}{\delta}\,. \tag{6.6}$$

Ideally, in numerical experiments, it is advisable to arrange for the probability of control to be close to unity, but if low success rates are unavoidable, then a possible factor of 2 that may be available from the choice of target string could be invaluable. Fig. 1(c) shows the result of numerical evaluation of the relative spread obtained from Eqs. (6.2) and (6.4) for the case when $\nu=1.000\,01$.

Equation (6.4) also provides information about how the correlation spread changes as the crisis is approached. As ν tends to unity, it can be shown that the peak in the spread of values of $p_{A_i}(\nu,r)$ essentially maintains its height and width while the maximum given by Eq. (6.5) moves monotonically to infinity. In this way, the range of values of r for which $p_{A_i}(\nu,r)$ is close to unity (and the relative spread is close to zero) expands until $p_{A_i}(1,r)\equiv 1$ for any A_i [cf. Eq. (6.2) with $z=\frac{1}{2}$].

B. Target interval dependence within an orbit

In a single-component experiment, in which the length of the target interval is fixed, there are q possible candidates for the target interval. It is clear that the numbers of preimages contributing to control occurring in exactly k iterations is determined by the correlation coefficients of the target code block and, therefore, these numbers can vary from one target interval to another. How does the probability of successful control depend on which of these intervals is chosen?

Consider the period-q orbit represented by the indefinite repetition of the string $00\ldots01$ (of length q) and each of its $q-1$ distinct cyclic permutations. The interval represented by the q-block $A_w=(.0\ldots010\ldots0)_q$, where w is the number of zeros to the *right* of the digit '1', contains one, and only one, of the period-q points. It is therefore a possible choice of target interval in a single-component experiment. Equation (2.15) can be used to obtain the generating function $G_{A_w}(z)$ for each $w=0,1,\ldots,q-1$, and the corresponding probabilities $p_{A_w}(\nu,q)=G_{A_w}((2\nu)^{-1})$ compared for different values of w.

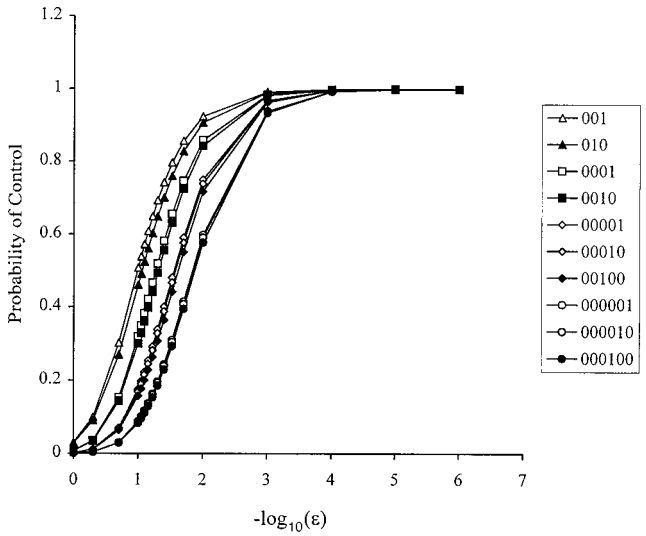

FIG. 2. Illustration of the intraorbit variation of the success rate of OGY control with the choice of target interval in a single-component experiment. Graphs show the values of the probability of successful control, $p_{A_w}(\nu,q)$, as $\epsilon=\nu-1$ approaches zero from above. Each plot corresponds to one of the possible choices of A_w in Eq. (6.8) when $q=3$, 4, 5, and 6. Recall that the probability of success is invariant under string reversal, i.e., $p_{A_w}(\nu,q)=p_{A_{q-1-w}}(\nu,q)$.

Each generating function is determined by the correlation coefficients of A_w and these indicator functions are invariant under reversal of the binary string defining the code block. Thus the correlation coefficients for A_w are the same as those of its reversal $\overline{A}_w=A_{q-1-w}$, so that $G_{A_w}(z)=G_{A_{q-1-w}}(z)$. It follows that it is sufficient to obtain $G_{A_i}(z)$ for $w=0,1,\ldots,w^*$, where

$$w^*=\begin{cases} q/2-1 & \text{if } q \text{ is even}\\ (q-1)/2 & \text{if } q \text{ is odd.}\end{cases} \tag{6.7}$$

Equation (2.15), together with Eqs. (2.14) and (2.2) (with $i=j$), gives

$$G_{A_w}(z)=G_{A_{q-1+w}}(z)=\begin{cases} z^q\{1-2z+z^q\}^{-1} & \text{for } w=0\\ z^q\left\{(1-2z)\left(1+\sum_{s=1}^{w}z^{q-s}\right)+z^q\right\}^{-1} & \text{for } w=1,\ldots,w^*.\end{cases} \tag{6.8}$$

Since the probability of successful control $p_{A_w}(\nu,q) = G_{A_w}((2\nu)^{-1})$, Eq. (6.8) shows that only for $\nu=1$ are all choices of target interval equally likely to achieve control in the single-component experiment. Although all choices for target interval have the same length, the correlations, which describe the ''first-entry'' property, affect the preimage numbers differently for each value of $w = 0,1,\ldots,w^*$. The results obtained by using Eq. (6.8) to calculate $p_{A_w}(\nu,q)$ for some trial values of ν and q are given in Fig. 2. It can be seen that measurable differences in success rates are to be expected. However, for the range of ν in Fig. 2, these differences are not sufficiently large for a significant advantage to be gained by choosing one target over another. Moreover, the spread of values over the orbit diminishes as q increases. It should be noted that the more rapid overall decline with increasing ν exhibited in Fig. 2 for higher q values is a result of the larger value of r in those cases. Recall that the length of the target is $(2\nu)^{-r}$, with $r=q$.

C. Target length dependence for a given orbit

The form of the r dependence of the probability of successful control to any choice of target block, and how it changes as the crisis is approached, was discussed in Sec. VI A. Similar behavior is to be expected for control to a particular period-q orbit ($q>1$) when a single-component target is used.

Consider the period-q point represented by the indefinite repetition of string 00 . . . 01 with q digits and focus attention on the target interval represented by $A_q=(.0\ldots01)_q$. This is one of q choices of target with length $(2\nu)^{-q}$ that exhibits symbolically one period of this period-q orbit. Symbolic representatives of smaller intervals that contain the same periodic point can be obtained by extracting longer blocks from the symbolic representation of the periodic orbit. For example, $A_{q+w}=(.0\ldots010\ldots0)_{q+w}$, with $w=1,2,\ldots,q-1$ zeros to the right of the digit '1', followed by $A_{2q}=(.0\ldots010\ldots01)_{2q}$, and so on. The general form for the generating function associated with a typical member of this sequence of code blocks is

$$G_{A_r}(z)=\begin{cases} z^r\left\{(1-2z)\left[\sum_{m=1}^{M} z^{(m-1)q}\right]+z^r\right\}^{-1} & \text{for } w=0 \\ z^r\left\{(1-2z)\left[\sum_{m=1}^{M} z^{(m-1)q}+\sum_{l=0}^{w-1} z^{Mq+l}\right]+z^r\right\}^{-1} & \text{for } w=1,\ldots,q-1, \end{cases} \tag{6.9}$$

where $r=Mq+w$ is the length of the block, with M a positive integer and $w=0,1,\ldots,q-1$.

Equation (6.9) gives the probability of successful control $p_{A_r}(\nu,r)=G_{A_r}((2\nu)^{-1})$ for the sequence of target intervals represented by the strings A_{Mq+w}. Some special cases are of interest. If $q=1$, then $M=r$ and $w=0$, so that only the first equation in (6.9) is required and the fixed point result of [1] is recovered. Note that this generating function is equal to $G_{LL}^{(r)}(z)$ given in Eq. (6.2) for each value of r. For each $q>1$, the lowest value of r in Eq. (6.9) is q ($M=1,w=0$) and the resulting generating function corresponds to $G_{UL}^{(q)}(z)$ given in Eq. (6.2). If q is increased to a value significantly greater than 1, then, for $z=(2\nu)^{-1}$, only the term with $m=1$ makes a numerically detectable contribution to the square brackets in Eq. (6.9) for any value of w. As a consequence, for q large enough, $p_{A_r}(\nu,r)\approx G_{UL}^{(r)}((2\nu)^{-1})$ for all r. This behavior is confirmed numerically in Fig. 3 for $\nu=1.000\,01$.

D. Average number of iterations to control when it occurs

The (ν,r) dependence of the average number of time steps before activation of the control to a period-q ($q>1$) orbit is qualitatively similar to that for the fixed point target reported in [1]. For example, calculations of $\tau_{A_r}(\nu,r)$ as a function of increasing r [i.e., target length $(2\nu)^{-r}$ decreasing] using Eq. (6.9) show that for $\nu>1$, this number reaches a finite limit, which increases as ν tends to 1; while, for $\nu=1$, it increases indefinitely. Sample results are shown in Fig. 4.

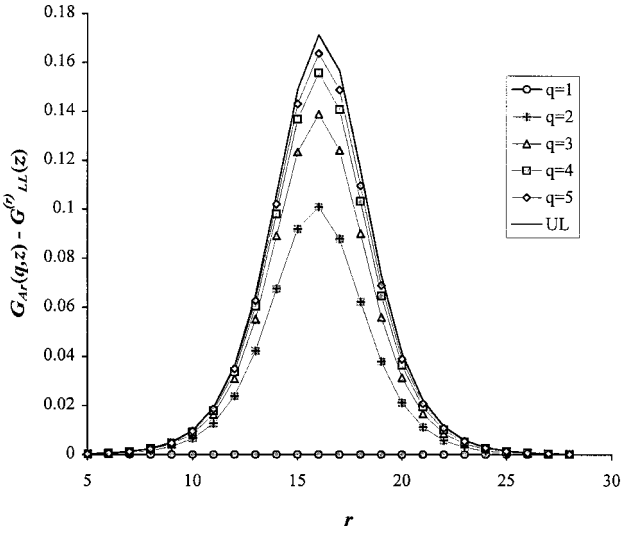

FIG. 3. Illustration of the relationship between $G_{A_r}(z)$ given by Eq. (6.9) and the limiting single-component generating functions of Eq. (6.2). The r dependence of $G_{A_r}(z)$, relative to the lower limit $G_{LL}^{(r)}(z)$, is shown for a fixed value of $z=1/(2\nu)$, with $\nu=1.000\,01$. Each graph corresponds to a single value of $q=1,2,3,4,5$. Observe that the r dependence of $G_{A_r}(z)$ approaches that of the upper limit $G_{UL}^{(r)}(z)$ as q increases.

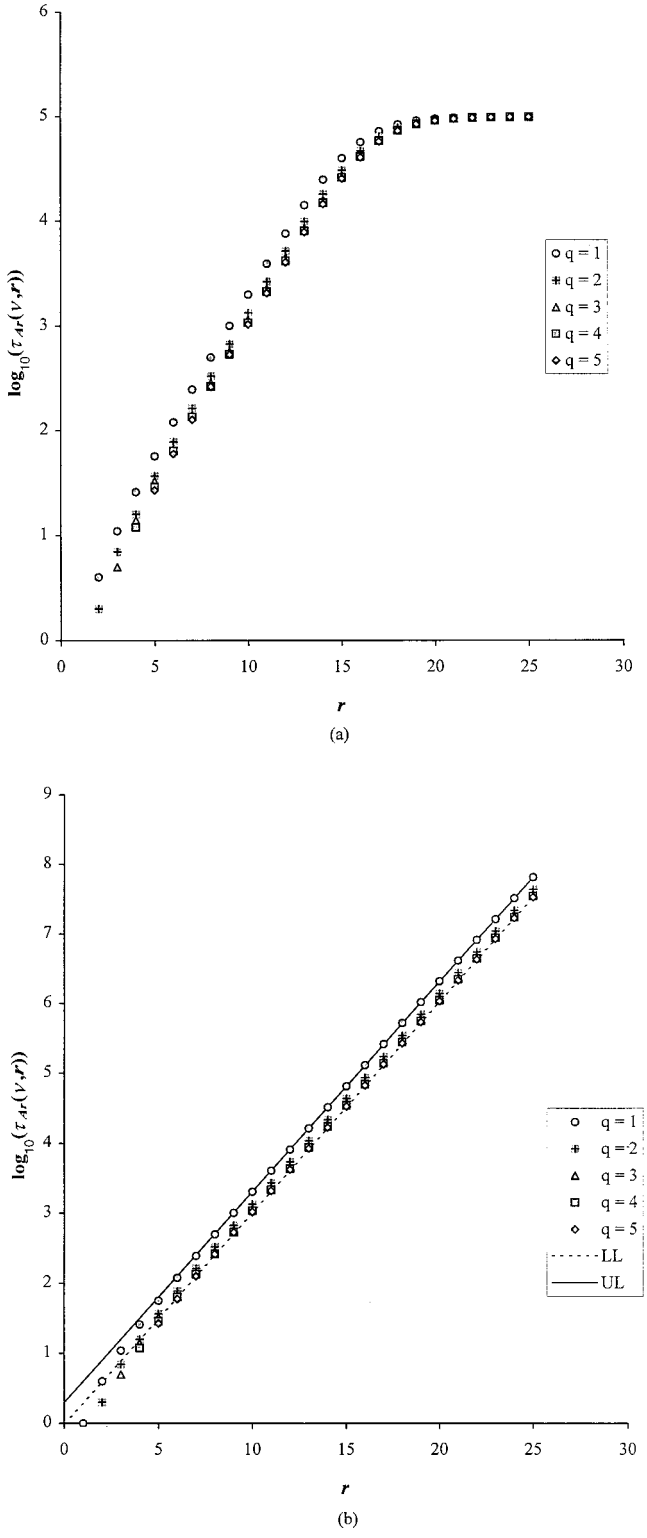

FIG. 4. Diagram illustrating the r dependence of the average number of iterations to control for the period-q orbits and single-component targets of the type discussed in Sec. VI C. Examples of numerical results obtained by using Eq. (6.9) to compute $\tau_{A_r}(\nu,r)$ as a function of $r=Mq+w$ for (a) $\nu=1.000\,01$ and (b) $\nu=1$ are presented. In both cases data are plotted for $q=1,2,3,4$, and 5.

The weak q dependence of the variation of $\tau_{A_r}(\nu,r)$ with r shown in Fig. 4 can be reconciled with the correlation polynomial limits introduced in Sec. VI A. For any single-component experiment target represented by the string A_i, Eq. (2.15) gives the generating function for the numbers of its preimages as

$$\hat{G}_{A_i}(z)=z^{-r}G_{A_i}(z)=\{(1-2z)C_{A_i}(z)+z^r\}^{-1} \quad (6.10)$$

and the specialization of Eq. (5.3) referred to in Sec. V B yields

$$\tau_{A_i}(\nu,r)=\left[\frac{z\hat{G}'_{A_i}(z)}{\hat{G}_{A_i}(z)}\right]_{z=(2\nu)^{-1}} =\left[\frac{z[2C_{A_i}(z)-(1-2z)C'_{A_i}(z)-rz^{r-1}]}{[(1-2z)C_{A_i}(z)+z^r]}\right]_{z=(2\nu)^{-1}}. \quad (6.11)$$

Since $z=(2\nu)^{-1}=2^{-1}(1-\delta)\leqslant 2^{-1}$, the terms rz^{r-1} and z^r decrease in magnitude rapidly as r increases and, when $\nu>1$, they can be neglected for r large enough. Thus Eq. (6.11) can be approximated by

$$\tau_{A_i}(\nu,r)\approx\left[\frac{z[2C_{A_i}(z)-(1-2z)C'_{A_i}(z)]}{(1-2z)C_{A_i}(z)}\right]_{z=(2\nu)^{-1}} =\frac{1-\delta}{\delta}-\left[\frac{zC'_{A_i}(z)}{C_{A_i}(z)}\right]_{z=(2\nu)^{-1}}. \quad (6.12)$$

It can be shown that the minimum (maximum) magnitude of the correlation dependent term in Eq. (6.12) is attained for the extreme polynomial $C_0(z)$ $[C_1(z)]$ given in Eq. (6.1), with the result that this term is bounded below by zero and above by $(1-\delta)/(1+\delta)$. Finally, it can be concluded that, for $\nu>1$,

$$\left(\frac{1-\delta}{1+\delta}\right)\frac{1}{\delta}\leqslant\lim_{r\to\infty}\tau_{A_i}(\nu,r)\leqslant\left(\frac{1-\delta}{\delta}\right). \quad (6.13)$$

Observe that both upper and lower bounds to the limiting value of τ converge to $1/\delta$ as $\delta\to 0$.

When $\nu=1$, the terms rz^{r-1} and z^r in Eq. (6.11) cannot be neglected, because z is then equal to $\frac{1}{2}$ and the factor of $(1-2z)=0$. In this case

$$\tau_{A_i}(1,r)=\left[\frac{z\{2C_{A_i}(z)-rz^{r-1}\}}{z^r}\right]_{z=2^{-1}} =2^rC_{A_i}(\tfrac{1}{2})-r, \quad (6.14)$$

and, when $2^r\gg r$, it follows that

$$\log_{10}[\tau_{A_i}(\nu,r)]=r\log_{10}(2)+\log_{10}[C_{A_i}(\tfrac{1}{2})]. \quad (6.15)$$

Equation (6.15) shows that a plot of $\log_{10}[\tau_{A_i}(\nu,r)]$ against r is asymptotically a straight line of slope equal to $\log_{10}(2)$ and intercept bounded by

$$0=\log_{10}[C_0(\tfrac{1}{2})]\leqslant\log_{10}[C_{A_i}(\tfrac{1}{2})]\leqslant\log_{10}[C_1(\tfrac{1}{2})]=\log_{10}(2). \tag{6.16}$$

This behavior is consistent with the numerical results given in Fig. 4(b), where the limiting straight lines given by Eqs. (6.15) and (6.16) are shown.

VII. DISCUSSION—MULTIPLE-COMPONENT TARGETS

The aim of this section is to provide an overview of the properties of multiple-component targets and to compare them with those of their single-component counterparts.

A. Qualitative properties of generating functions

1. $\nu>1$

The equations (2.7) and (2.8) defining the generating functions associated with the individual components of the target union can be used to show that their sum $H_{L_q}(z)$ takes a form similar to that of $G_{A_i}(z)$ given in Eq. (2.15). The result of substituting Eq. (2.8) into Eq. (2.7) can be written in the matrix form

$$\mathbf{C}(z)\mathbf{H}(z)=z^r\left\{\frac{1-S(\mathbf{H}(z))}{1-2z}\right\}\mathbf{J}=\gamma(z)\mathbf{J}, \tag{7.1}$$

where $\mathbf{H}(z)=[H_{L_q}^{(1)}\cdots H_{L_q}^{(q)}]^T$, $\mathbf{J}=[1\cdots1]^T$ are $(q\times1)$ vectors, $S(\mathbf{H}(z))=\Sigma_{j=1}^{q}H_{L_q}^{(j)}(z)=H_{L_q}(z)$, and $\mathbf{C}(z)=[C_{ij}(z)]_{i,j=1}^{q}$. Given that $\mathbf{C}(z)$ is nonsingular, Eq. (7.1) implies

$$H_{L_q}(z)=S(\mathbf{H}(z))=\frac{z^r}{\{(1-2z)S(\mathbf{Y}(z))^{-1}+z^r\}}, \tag{7.2}$$

where $\mathbf{Y}(z)=\mathbf{C}(z)^{-1}\mathbf{J}$. In the special case $q=1$, $S(\mathbf{Y}(z))^{-1}=C_{A_i}(z)$ and Eq. (2.15) is recovered explicitly from Eq. (7.2). Thus, provided the inverse matrix $\mathbf{C}(z)^{-1}$ exists and the sum of its elements (the product with $\mathbf{J}$ forms row sums and the function S sums these) is not equal to zero for $z=(2\nu)^{-1}=2^{-1}(1-\delta)$, with small $\delta\geqslant0$, Eq. (7.2) shows that the qualitative behavior of the probability that control will occur is the same as that for the single-component target. Moreover, it also follows that, under the same conditions, this statement will be true of the average number of iterations to control when it occurs (cf. Sec. VI 1).

2. $\nu=1$

This case corresponds to $z=\frac{1}{2}$, when Eqs. (2.7) and (2.8) give $H_{L_q}(\frac{1}{2})=1$. However, the numbers $h(j,m)$, and therefore $H_{L_q}^{(j)}(\frac{1}{2})=\Sigma_{m=0}^{\infty}h(j,m)2^{-m}$, are still well defined for $j=1,\ldots,q$, provided that the summation converges. Values for $H_{L_q}^{(j)}(\frac{1}{2})$ can be extracted from Eq. (7.1) by assuming that the z derivative $D_zH_{L_q}(\frac{1}{2})\neq0$ and taking the limit $\delta\to0$. The result is

$$\mathbf{C}(\tfrac{1}{2})\mathbf{H}(\tfrac{1}{2})=2^{-(r+1)}D_zH_{L_q}(\tfrac{1}{2})\mathbf{J}=\gamma(\tfrac{1}{2})\mathbf{J}. \tag{7.3}$$

However, it is known that $S(\mathbf{H}(\frac{1}{2}))=H_{L_q}(\frac{1}{2})=1$, so that Eq. (7.3) yields $\mathbf{H}(\frac{1}{2})=\gamma(\frac{1}{2})\mathbf{Y}(\frac{1}{2})$ where $\mathbf{Y}(\frac{1}{2})=\mathbf{C}(\frac{1}{2})^{-1}\mathbf{J}$ and $\gamma(\frac{1}{2})=S(\mathbf{Y}(\frac{1}{2}))^{-1}$.

The quantities $H_{L_q}^{(j)}(\frac{1}{2})$, for $j=1,\ldots,q$, are the probabilities of first entry into the target union L_q at A_j. The following example shows that these probabilities depend on j. Consider control to the period-3 orbit represented by indefinite repetition of the string 001 using the target union $L_3=\{A_1,A_2,A_3\}$, where $A_1=(001001)$, $A_2=(010010)$, and $A_3=(100100)$. The correlation polynomials for these target component strings can be obtained from Eq. (2.6), by using Eq. (2.2), and the correlation matrix $\mathbf{C}(\frac{1}{2})$ constructed. Solution of Eq. (7.3) then gives

$$\begin{aligned}H_{L_3}^{(1)}\left(\frac{1}{2}\right)&=0.326\,037,\\ H_{L_3}^{(2)}\left(\frac{1}{2}\right)&=0.331\,797,\\ H_{L_3}^{(3)}\left(\frac{1}{2}\right)&=0.342\,166,\end{aligned} \tag{7.4}$$

to six decimal places. The differences recorded in Eq. (7.4) are not large, but they show that the effect of different correlations between the strings representing the components of the target is to create an asymmetry between the probabilities of first entry at the individual components of the target union.

B. Numerical evaluation of generating functions

Quantitative results can be obtained directly from Eqs. (2.7) and (2.8) for any chosen periodic orbit and any target union containing it. For a particular value of $z=(2\nu)^{-1}$, Eq. (2.7) provides a set of linear equations for the unknown values $H_{L_q}^{(j)}((2\nu)^{-1})$, $j=1,\ldots,q$ (cf. Sec. VII A 2, where $\nu=1$). However, to examine the approach to the crisis it is more convenient to use one of the many computer algebra software packages (such as MATHEMATICA or MAPLE) to obtain the rational functions of z that satisfy Eq. (2.7) and to simply evaluate these forms for whatever values of z are required. Knowledge of the numerator and denominator polynomials of the rational generating function $H_{L_q}(z)$ allows Eq. (5.3) to be used to compute the average number of iterations to control (when it occurs) for the chosen target union. By way of illustration, the generating functions associated with control to the period-3 orbit considered in Sec. VII A 2 are presented here.

For the target union $L_3=\{A_1,A_2,A_3\}$, the coefficient polynomials $\pi_{ij}(z)$ in Eq. (2.7) can be derived from the correlation polynomials given by Eqs. (2.6) and (2.2). The solution of Eq. (2.7) using MATHEMATICA 4.0 is

$$H_{L_3}^{(1)}(z)=\frac{z^6(1-z+z^3-z^4-z^6+z^7-z^9)}{1-2z+z^3-2z^4+z^5-z^6+z^7+z^8-z^9+z^{10}+z^{13}}, \tag{7.5}$$

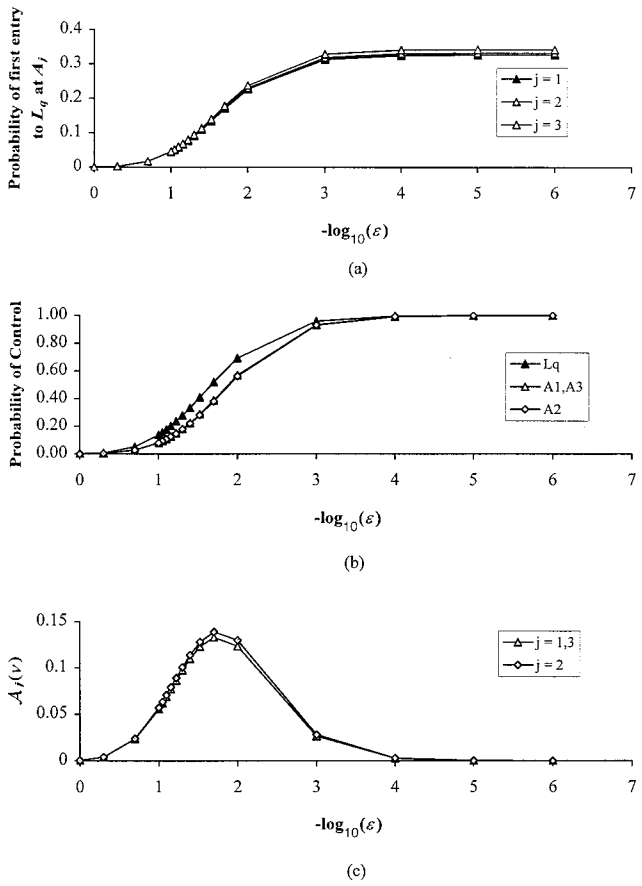

FIG. 5. Plots showing (a) the probability of first entry into the target union $L_3=\{A_1,A_2,A_3\}$ at each of its three disjoint components, (b) the probability of successful control using L_3 in relation to the corresponding probabilities for single-component targets A_1,A_2,A_3, (c) the advantage, $\mathcal{A}_j(\nu)=H_{L_3}(z)-G_{A_j}(z)$, $z=1/(2\nu)$, gained by the multiple-component target over its single-component counterparts, as functions of $\epsilon=\nu-1$.

$$H_{L_3}^{(2)}(z)=\frac{z^6(1-z+z^3-z^4)}{1-2z+z^3-2z^4+z^5-z^6+z^7+z^8-z^9+z^{10}+z^{13}}, \tag{7.6}$$

$$H_{L_3}^{(3)}(z)=\frac{z^6(1-z+z^3-z^4+z^5-z^6+z^8-z^9)}{1-2z+z^3-2z^4+z^5-z^6+z^7+z^8-z^9+z^{10}+z^{13}}. \tag{7.7}$$

The numerator and denominator polynomials in Eqs. (7.5)–(7.7) are relatively prime and all three share the same denominator. For $\nu=1$, the values of $H_{L_q}^{(j)}(\frac{1}{2})$, for $j=1,2,3$, obtained from Eqs. (7.5)–(7.7) with $z=\frac{1}{2}$, are precisely those given in Eq. (7.4). Figure 5(a) shows plots of $H_{L_q}^{(j)}((2\nu)^{-1})$, $j=1,2,3$, for some trial values of $\nu>1$. It can be seen that all three quantities fall toward zero as ν increases. The corresponding values of the probability $p_{L_q}(\nu,r)=H_{L_q}((2\nu)^{-1})$, obtained by summing over j, are shown in Fig. 5(b) together with data obtained when each of the intervals of the target union is used as a single-component target. Figure 5(c) compares the multiple- and single-component target results by showing the ν dependence of the ''advantage'' of the former over the latter. The advantage passes through a maximum value approximately equal to 0.14 for $\nu\approx1.02$ and falls to

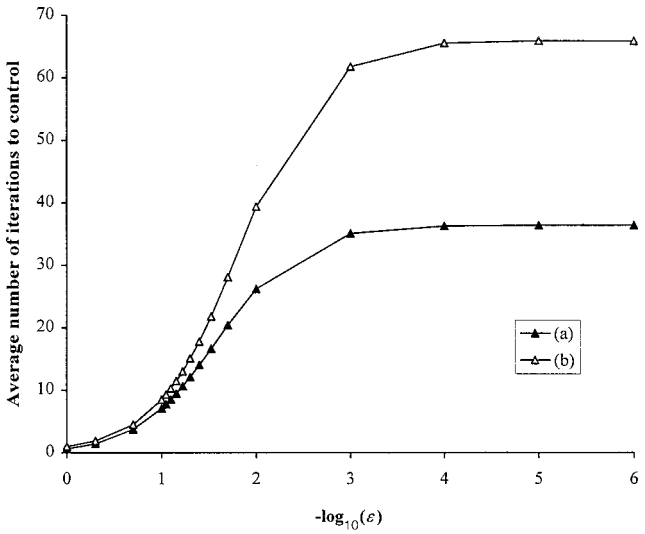

FIG. 6. Comparison of the average number of iterations to control for the period-3 orbit using (a) the target union L_3 and (b) the target interval A_1 as a function of the distance from the crisis measured by the negative, base-10 logarithm of $\epsilon=\nu-1$.

values near zero for (a) ν significantly different from 1, and (b) ν tending to 1. The trend in (a) comes from the reduction in all preimage lengths that occurs when ν increases, with the result that the probability of successful control falls to zero in both types of experiment. The behavior in (b) follows because the probability of successful control tends to unity in both multiple- and single-component experiments, as ν approaches 1.

Figure 5 suggests that there is little advantage to using a multiple-component target, particularly in the immediate vicinity of the crisis. For such values of ν both multiple- and single-component experiments succeed in reaching their targets with probability close to 1, but the average number of iterations to control (when control occurs) can be significantly smaller when a multiple-component target is used. Equations (7.5)–(7.7) can be used to obtain $\hat{H}_{L_3}(z)$ [cf. Eq. (5.1)] for the period-3 orbit to which they refer. Equation (5.3) then allows the average number of iterations to control, $\tau_{L_3}(\nu,6)$, for that orbit to be calculated. The corresponding single-component quantities, $\tau_{A_i}(\nu,6)$, $i=1,2,3$, can be obtained using the correlation polynomials given by Eq. (2.14) in conjunction with Eqs. (6.10) and (6.11). Computed values of $\tau_{L_3}(\nu,6)$ and $\tau_{A_1}(\nu,6)$ are compared in Fig. 6. The values of $\tau_{A_i}(\nu,6)$ do not depend strongly on i, and, indeed, are the same for $i=1$ and 3. It can be seen that, for ν near 1, the multiple-component target leads to a significant improvement in the average waiting time to control in this example.

C. Application of recurrence relations

The generating functions discussed in Sec.VII A provide the probability of successful control, and the average number of iterations to control, in the limit of arbitrarily large numbers of iterations. The analysis of Sec. IV provides explicit values for the numbers of first-entry preimages of finite order and this can be used to compare the effectiveness of multiple- and single-component targets for finite numbers of

TABLE II. Comparison of first-entry preimages given by Eq. (7.9) with their single-component counterparts for selected values of the order k.

k	$N_k^{(6)}(L_3)$	$N_k^{(6)}(A_1)$	$N_k^{(6)}(A_2)$	A_1/L_3 (%)	A_2/L_3 (%)
0	3	1	1	33.33	33.33
1	3	2	2	66.67	66.67
2	6	4	4	66.67	66.67
3	12	7	7	58.33	58.33
4	24	14	14	58.33	58.33
5	46	28	27	60.87	58.70
6	90	56	54	62.22	60.00
7	175	110	106	62.86	60.57
8	341	216	210	63.34	61.58
9	664	425	413	64.01	62.20
10	1293	838	815	64.81	63.03
20	1015143	738864	721171	72.28	71.04
30	796960021	651164399	638552724	81.71	80.12

iterations. The example of control to a period-3 orbit, introduced in Sec.VII A, can be used to illustrate the results of calculations of this kind.

The correlation coefficients for the strings $A_1=(001001)$, $A_2=(010010)$, and $A_3=(100100)$ are given by Eq. (2.2), and the numbers of first-entry preimages for each of the components of the target union $L_3=\{A_1,A_2,A_3\}$ are obtained by substituting them into Eq. (4.2). For example, when $i=1$, Eq. (4.2) gives

$$\begin{aligned} h_{L_3}(1,m+1)=&2h_{L_3}(1,m)-h_{L_3}(1,m-2)+2h_{L_3}(1,m-3)\\ &-h_{L_3}(1,m-5)-h_{L_3}(2,m-1)+2h_{L_3}(2,m\\ &-2)-h_{L_3}(2,m-4)+h_{L_3}(2,m-5)\\ &-h_{L_3}(3,m)+2h_{L_3}(3,m-1)-h_{L_3}(3,m-3)\\ &+h_{L_3}(3,m-4)+h_{L_3}(3,m-5) \end{aligned} \tag{7.8}$$

for $m=k+r\geq 6$. Observe that the right-hand side of Eq. (7.8) includes numbers $h_{L_3}(j,m-s)$ with $j=2$ and 3 in addition to those with $j=i=1$. Such ''cross-correlation terms'' do not appear in the recurrence relations associated with single-component targets but are a feature of the multiple-component case. Initial conditions for the use of Eq. (7.8), and the equations arising from Eq. (4.2) when $i=2$ and 3, are $h_{L_3}(i,m)=0$, $m=1,\ldots,5$, $h_{L_3}(i,6)=1$, $i=1,2,3$. Of course, the quantity of interest in the multiple-component experiment is the sum over i of the number of preimages corresponding to first-entry at component i of the target union, i.e.,

$$N_k^{(6)}(L_3)=\sum_{i=1}^{3} h_{L_3}(i,k+6), \tag{7.9}$$

for $k=0,1,\ldots$. Moreover, it is this number that is to be compared with the single-component counterparts obtained by substituting the diagonal (or ''self-'') correlation coefficients into Eq. (4.3) to obtain $N_k^{(6)}(A_i)=g_{A_i}(k+6)$, for $k=0,1,\ldots$ and $i=1,2,3$. Table II contains such comparative data for some selected values of k. Note that $N_k^{(6)}(A_3)=N_k^{(6)}(A_1)$ (because $A_3=\overline{A_1}$) while $N_k^{(6)}(A_2)$ is slightly smaller (because the self-correlation coefficients of A_2 are different from those of A_1 and A_3). Although $N_k^{(6)}(L_3)$ dominates $N_k^{(6)}(A_i)$, particularly at low k, the growth rates of the recurrence relations are different and both sequences of numbers have the property that their sums, when weighted with the $\nu=1$ preimage lengths of $2^{-(k+6)}$, are unity. More generally, the partial sums (to n terms) of both sequences, when weighted with the $\nu>1$ pre-image lengths $(2\nu)^{-(k+6)}$, give the probabilities $p_{L_3}(\nu,6;n)$ and $p_{A_i}(\nu,6;n)$ of successful control in less than or equal to n iterations. The advantage, $\mathcal{A}_i(\nu,n)$, of the multiple-component target over the single-component target can then be defined by

$$\begin{aligned} \mathcal{A}_i(\nu,n)&=p_{L_3}(\nu,6;n)-p_{A_i}(\nu,6;n)\\ &=\sum_{k=0}^{n}[N_k^{(6)}(L_3)-N_k^{(6)}(A_i)](2\nu)^{-(k+6)}. \end{aligned} \tag{7.10}$$

In the limit $n\to\infty$, the summation in Eq. (7.10) converges to the limiting advantages shown in Fig. 5(c). The form of the n dependence of $\mathcal{A}_i(\nu,n)$ changes significantly as ν approaches unity from above (see Fig. 7). The weak i dependence of $\mathcal{A}_i(\nu,n)$ is not important here and attention is focused on the single-component data for A_2. For $\nu=1$, the advantage associated with the multiple-component target passes through a well-defined maximum of about 0.22 when n is approximately 50. As ν increases above 1, the height of this maximum declines and its definition deteriorates until, for $\nu=1.05$, only a ''shoulder'' remains and the advantage of the multiple-component target is essentially constant for $n>50$. The number differences in Eq. (7.10) are independent of ν and therefore the behavior shown in Fig. 7 reflects a shift in weight away from the lower values of k in Eq. (7.10)

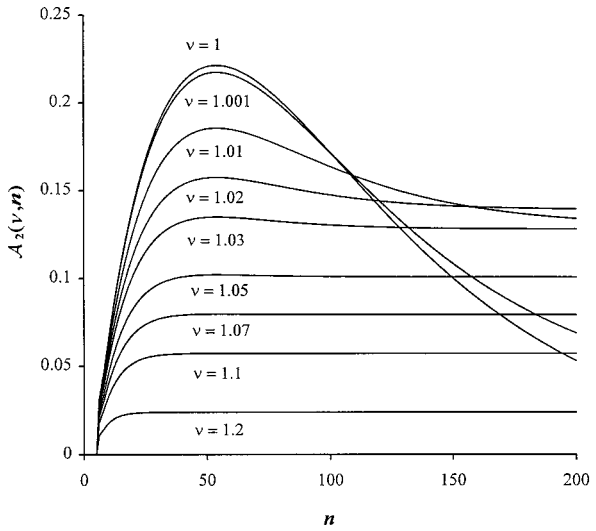

FIG. 7. Numerical results showing how the n dependence of $\mathcal{A}_2(\nu,n)$ changes as ν increases above 1. For the values of ν used in this diagram, the limiting values of the multiple-component advantage as n tends to infinity are given in Fig. 5(c).

as ν increases. Thus significant gains in probability of successful control to a nontrivial periodic orbit can be achieved by using a multiple-component target provided ν is sufficiently close to unity. Moreover, in the present example, such gains occur at relatively small numbers of iterations.

VIII. CONCLUSION

The combinatorial techniques used in [1] to treat the statistics of OGY control to the nontrivial fixed point of transiently chaotic tent maps have been extended to period-q orbits with $q>1$. Two types of statistical experiment have been analyzed: (a) multiple-component experiments in which the periodic orbit is accessed through a target consisting of the union of q disjoint intervals each containing one of the q periodic points; and (b) single-component experiments in which a single interval containing any one of the periodic points is targeted. As in [1], the aim is to count the numbers of first-entry preimages of the symbolically defined target interval or union. Given the binary string(s) defining the target, a closed form can be obtained for the generating function for the required preimage numbers, which, in turn, yields the probability of control taking place and the average number of iterations to control when it occurs. Recurrence relations for the numbers of first-entry preimages of the target allow calculation of the probability of control occurring in less than or equal to a chosen number of iterations. The results for experiments of type (a) are complicated by the appearance of cross correlations between the strings representing the different components of the target union.

The tent map itself ($\nu=1$) is a prototype of chaotic behavior and the crisis of its chaotic attractor that occurs in the family of tent maps ($\nu\geqslant 1$) studied here is representative of the behavior of other families of unimodal maps. The symbolic approach to the application of the OGY strategy to transiently chaotic tent maps allows an exact treatment of control to nontrivial periodic orbits to be developed for this important paradigm. The results obtained allow a formal study of the design of numerical experiments that can act as a valuable guide to dealing with models where exact solutions are not available and statistical experiments provide the only feasible approach. This aspect of the work presented in [1] has been discussed in [7]. Here it has been illustrated by comparing the properties of experiments of types (a) and (b). The absence of cross correlations between different components of the target union means that the analysis based on a single target interval is better suited to questions involving a range of values of q or r. In such cases, generating functions are easily obtained without recourse to computer algebra, and recurrence relations can be iterated within a single row or column of an array. The examples considered indicate that the qualitative behavior of the probability of control, and the number of iterations to control, are the same for both types of target, and that quantitative differences arising from correlation effects are of secondary importance for single-component targets. However, significant gains in both the practical success rate and the number of iterations to control can be achieved by using the multiple-component target when the operational conditions are sufficiently close to the crisis.

It is important to note that combinatorial aspects of the symbolic analysis presented above are determined solely by the symbolic dynamics of the system at the crisis. Consequently, the preimage numbers obtained at a given order are equally valid for maps other than the tent map that have the same symbolic representation. The difficulty in using these results to obtain information about such maps is that, in general, the preimage lengths are then not the same for all preimages of a given order. The simple transition from first-entry, order-k preimage numbers to a probability density at order k by multiplying by the preimage length is no longer valid. However, the symbolic approach clearly admits an exact treatment of the ''first-entry'' aspect of the application of the OGY strategy to unimodal maps near crisis, and work on the translation of this information into statistical parameters for more general unimodal maps continues.

[1] C.M. Place and D.K. Arrowsmith, preceding paper, Phys. Rev. E **61**, 1357 (2000).
[2] T. Tél, J. Phys. A **24**, L1359 (1991).
[3] C. Romeiras, C. Grebogi, E. Ott, and W.P. Dayawansa, Physica D **58**, 165 (1992).
[4] P. So and E. Ott, Phys. Rev. E **51**, 2955 (1995).
[5] A.M. Odlyzko, in *Handbook of Combinatorics*, Vol. 2, edited by R.L. Graham, M. Grötschel, and L. Lovász (Elsevier Science B.V., Amsterdam, 1995), Chap. 22.
[6] L.J. Guibas and A.M. Odlyzko, J. Comb. Theory, Ser. A **30**, 183 (1981).
[7] C.M. Place and D.K. Arrowsmith, Interim Report, Mathematics Research Centre, School of Mathematical Sciences, Queen Mary & Westfield College, London (unpublished).